In Situ Synthesis, Magnetic Property, and Formation Mechanism of Fe_3O_4 Particles Encapsulated in 1D Bamboo-Shaped Carbon Microtubes

Liqiang Xu,*,† Jin Du,‡ Peng Li,† and Yitai Qian†,‡

Key Laboratory of Colloid and Interface Chemistry, Shandong University, Ministry of Education, P.R. China, and Department of Chemistry, University of Science and Technology of China, Hefei, Anhui 230026, P.R. China

Fe_3O_4 particles embedded in bamboo-shaped carbon microtubes (defined as "BCIOs") with ferromagnetic properties were in situ produced by redox reactions between ferrocene and glycerol in a stainless steel autoclave of 20-mL capacity at 600 °C; these BCIOs have wide and periodic variable outer diameter distributions and have lengths up to tens of micrometers. It is found that their coercivity values were in inverse ratio with the sizes of interior Fe_3O_4 particles when compared with the previous reports. After the acid treatment process, bamboo-shaped carbon microtubes could also be obtained, while when a contrasting experiment was carried out in a stainless steel autoclave of 60-mL capacity, only irregular-shaped Fe_3O_4 particles encapsulated in carbon capsule core−shell composites were produced. On the basis of the experimental results, the possible formation processes of these as-obtained products were discussed.

Introduction

Recently, magnetic iron oxides encapsulated in carbon nanotubes (CNTs) or carbon microtubes (CMTs) based systems have attracted increasing attention due to their electric and magnetic properties and their variety of potential technological applications.[1−3] Of all known iron oxides, Fe_3O_4 exhibits by far the most interesting properties based on the presence of Fe cations in two valence states: the divalent Fe^{2+} ion and the trivalent Fe^{3+} ions (Fe_3O_4 can be written in the form $[Fe^{3+}]_A[(Fe^{2+},Fe^{3+})]_BO_4$, in which A is tetrahedral sites and B is octahedral sites), which has potential uses in industry such as in catalysis, magnetic data storage, ferrofluids, and spin electronic devices due to its intrinsic half-metallic ferromagnetic nature.[4,5] Fe_3O_4 nanoparticles have been investigated for various applications owing to their stability and nontoxic property;[6,7] however, because of anisotropic dipolar attraction, nanometer-sized Fe_3O_4 cores tend to aggregate into larger clusters, which result in losing the specific properties associated with their nanometer dimensions; therefore, the manufacturing of Fe_3O_4 nanoparticles separated by nonmagnetic material has become attractive for possible use in the development of modern electronics. To date, Fe_3O_4 nanoparticles encapsulated in normal carbon tube systems have been frequently investigated;[1,8] however, to our knowledge, there are few reports in the literature about the preparation and magnetic property investigation of Fe_3O_4 particles fully encapsulated in one-dimensional (1D) bamboo-shaped CMTs up to now. Compared with uniform carbon tubes, bamboo-shaped carbon tubes (BCTs) have the unique characteristics that their inner cavum are constructed by many separated hollow compartments, which could be utilized as the ideal containers for loading magnetic particles such as Fe_3O_4 particles in their hollow compartments to prevent them from agglomerating when a magnetic field is not applied and

to restrict their movement utilizing their special structures. BCTs have been extensively studied to explore their unique structure-associated properties and to understand the relationship between their formation and the growth of normal carbon tubes that exhibit continuous hollow channels, and they are extremely promising for applications in electronic devices.[9,10] BCTs have been fabricated through various processes by means of arc discharge,[11,12] pyrolysis of organometallic compounds,[13−15] thermal chemical vapor deposition (CVD),[16] microwave plasma-enhanced CVD, etc.[17,18] In this report, 1D bamboo-shaped Fe_3O_4 particles fully encapsulated in CMTs core−shell composites were prepared for the first time via a direct one-step solvothermal process by pyrolysis of the mixture of ferrocene and glycerol in an autoclave of 20-mL capacity at 600 °C. In addition, hollow bamboo-shaped CMTs could be easily obtained after the inner Fe_3O_4 particles were removed by the acid treatment process, while when a contrasting experiment was carried out in a stainless steel autoclave of 60-mL capacity, only irregular-shaped Fe_3O_4 particles encapsulated in carbon capsule core−shell composites were produced, similarly, hollow carbon capsules could also be obtained. This approach provides a simple and facile approach to produce 1D BCIOs, hollow bamboo-shaped CMTs, and hollow carbon capsules. The formation processes of these as-synthesized products were discussed according to the experimental results. This report is a further progress of our previous works.[19,20]

Experimental Section

Sample Preparation. In a typical procedure, ferrocene (1.0 g) and glycerol (18 mL) were mixed homogeneously and were loaded into a stainless steel autoclave of 20-mL capacity (the filling ratio was about 90%). The autoclave was sealed and put into an electronic furnace at room temperature. The temperature of the furnace was increased from room temperature to 600 °C in 60 min and maintained at 600 °C for 16 h, and then it was allowed to cool to room temperature naturally. The dark precipitates (labeled as Sample 1) in the autoclave were collected

* To whom correspondence should be addressed. Phone: +86-531-88364543. Fax: +86-531-88366027. E-mail: xulq@sdu.edu.cn.
† Shandong University.
‡ University of Science and Technology of China.

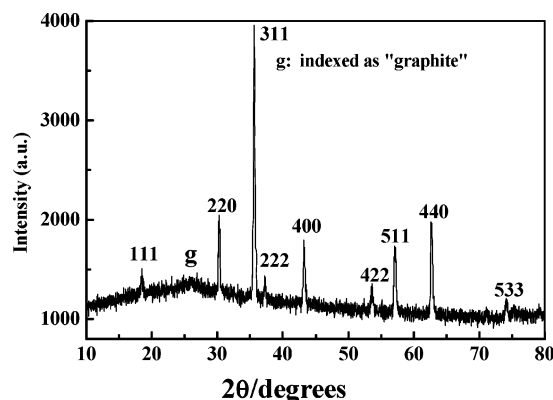**Figure 1.** XRD pattern of Sample 1 obtained before the acid treatment process.

Figure 2. Micro-Raman spectrum of Sample 1 obtained after the acid treatment process.

and divided into two parts: one part of Sample 1 was washed with distilled water and absolute ethanol several times to obtain the BCIOs; the other part was heated in dilute HCl acidic solution at 80 °C for 24 h to obtain the bamboo-shaped CMTs. After that these products were dried in a vacuum box at 60 °C for 4 h and were collected for characterization. In a contrasting experiment, a 60-mL capacity stainless steel autoclave was used instead of the 20-mL capacity autoclave (the filling ratio was about 30%). These as-obtained products were labeled as Sample 2.

Sample Characterization. X-ray powder diffraction (XRD) patterns of the products were recorded on a Philips X'pert diffractometer with Cu Kα radiation ($\lambda = 1.5418$ Å). A micro-Raman spectrum of Sample 1 (after the acid treatment process) was taken at room temperature on a SPEX 1403 spectrometer with an argon-ion laser at an excitation wavelength of 514.5 nm. The morphology of the products was investigated by field emission scanning electron microscopy (FSEM, JEOL JSM-6300F). Structural characterizations were done by transmission electron microscopy (TEM, HITACHI 800) and high-resolution TEM (HRTEM, JEOL 2010 using an accelerating voltage of 200 kV). Magnetic hysteresis loops studies were performed at room temperature by first saturating Sample 1 (without acid treatment) in a field of 10 000 Oe, then the saturation magnetization (M_s), the remanent magnetization (M_r), and the coercivity (H_c) were determined for the sample.

Results

The XRD pattern of Sample 1 obtained before the acid treatment process is shown in Figure 1; the analysis result indicates that the product was composed of two phases: the broadened peaks with relatively low peak intensity could be ascribed to the diffraction of graphite, the other sharp peaks with relatively high peak intensity could be indexed as face-centered cubic (fcc) Fe_3O_4 (JCPDS card No.19-629). The XRD pattern of Sample 1 obtained after the acid treatment process was only composed of broad peaks that could be indexed as graphite, which indicates that Fe_3O_4 could be thoroughly removed after the acid treatment process and led to a quite pure carbon phase; Figure 2 shows the micro-Raman spectrum of Sample 1 obtained after the acid treatment; it is observed that there are two sharp peaks at about 1330 (D-band) and 1597 cm^{-1} (G-band), respectively. The intensity ratio of D- to G-band (I_D/I_G) is about 0.62, which reveals the relatively high crystallinity of the as-obtained carbon materials.

Magnetic properties of Sample 1 without the acid treatment course were measured at room temperature. The hysteresis loop of the products shown in Figure 3 reveals a ferromagnetic
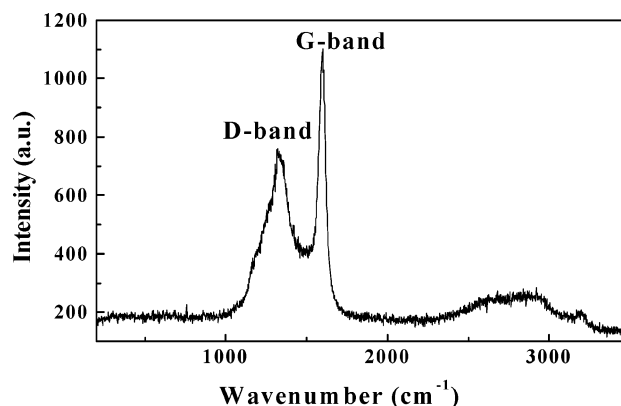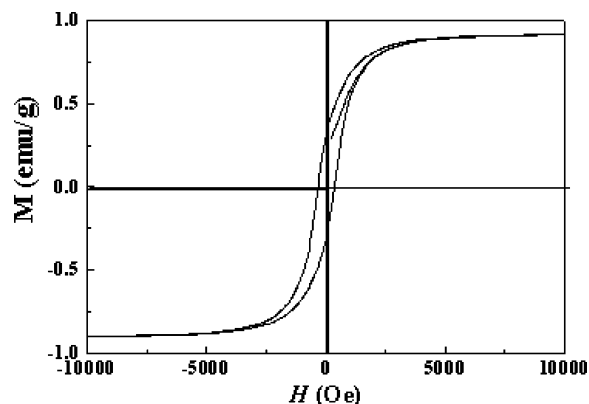

Figure 3. Magnetic hysteresis loop of Sample 1 (without undergoing the acid treatment course) measured at room temperature.

behavior with saturation magnetization (M_s), remanent magnetization (M_r), and coercivity (H_c) values of ca. 0.91 emu/g, 0.31 emu/g and 325.6 Oe, respectively, and the values of the M_s are much lower than those of the Fe_3O_4 nanoparticles and our previously reported Fe_3O_4 encapsulated in carbon core−shell structures;[19−21] it is considered that the remarkable decrease of M_s values that occurred in this experiment might be attributed to the wide existence of graphitic layers on the surface of the Fe_3O_4 particles, which result in the formation of many Fe_3O_4 particles encapsulated in carbon core−shell subunits with relative low order arrangement. These graphitic layers in such structured subunits restrict the optional movement and interactions of the Fe_3O_4 particles, as can be seen in Figure 4d,h. Its role is similar to that of the surfactant that existed on the surface of Fe_3O_4 nanoparticles, which leads to decreased M_s values;[21−22] however, the exact reason still needs further investigation. Compared with our previous reports, it is found that the coercivity (H_c) values were in inverse ratio with the sizes of Fe_3O_4 particles,[19,20] and this result obtained in our experimental cases is consistent with the literature reports about the relationships between the H_c values and the diameters of Fe_3O_4 particles (when the diameter of Fe_3O_4 particles is in the range of 100−300 nm).[23]

The results of FSEM, TEM, HRTEM, and SAED pattern analyses indicate that Sample 1 obtained without acid treatment were composed of 1D BCIOs and solid carbon microspheres, and the yield of 1D BCIOs core−shell composite was about 70% according to the FSEM and TEM statistic observation analyses results. Parts a and b of Figure 4 show FSEM images of the as-obtained bamboo-shaped product, which are all in one-dimensional forms. It is also quite remarkable that these products have a periodic and extended range of diameters along their
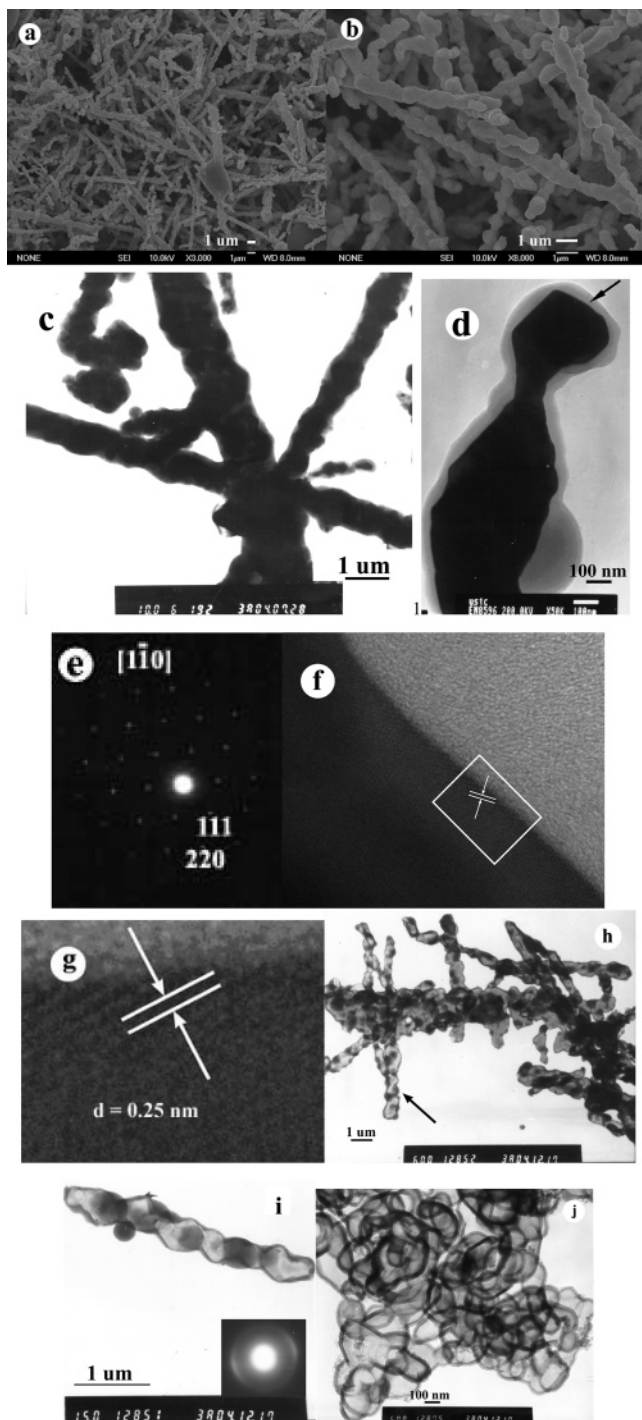
Fe$_3$O$_4$ Particles in Bamboo-Shaped Carbon Microtubes

J. Phys. Chem. B, Vol. 110, No. 9, 2006 **3873**

Figure 4. Representative FSEM, TEM, and HRTEM images and the corresponding SAED patterns of Sample 1 obtained before (a−g) and after acid treatment (h, i), respectively; (j) TEM image of Sample 2 obtained after the acid treatment process.

lengths, which look like bamboo observed from its exterior morphology, and their lengths were up to tens of micrometers. This is quite different from the characteristics of the previously widely reported bamboo-shaped carbon nanotubes (they usually have almost the same exterior diameters along their lengths). In addition, these BCIOs have smooth surfaces and have both tips closed as observed from the magnified FSEM images. Figure 4c shows a typical TEM image of Sample 1 obtained before the acid treatment course; it is clear that each of the bamboo-shaped 1D composites is composed of two kinds of material: graphite and Fe$_3$O$_4$. It is worth noting that a large

portion of the Fe$_3$O$_4$ is in nanoparticle form, and these Fe$_3$O$_4$ nanoparticles are blocked off by the graphite and form many separate units, which is different from our previously reported cable-like Fe$_3$O$_4$ nanowires encapsulated in CMTs.[19] A typical TEM image of a single core−shell composite is shown in Figure 4d, which reveals that neither the diameter of the Fe$_3$O$_4$ nanoparticles nor the thickness of the graphite layer is uniform, and these Fe$_3$O$_4$ nanoparticles are joined together at one tip of a single BCIO. Its corresponding SAED pattern and HRTEM images are shown in Figure 4e−g. As the graphite layer is extremely thin, therefore, we could only observe clear diffraction spots that belong to the diffraction of Fe$_3$O$_4$ nanoparticles. Its corresponding SAED pattern is shown in Figure 4e; the clear and sharp diffraction spots can be indexed as 11$\bar{1}$, 111, and 220 diffractions of fcc Fe$_3$O$_4$ with a zone axis of [1$\bar{1}$0], which reveals that the inner Fe$_3$O$_4$ particles are well crystallized. Parts f and g of Figure 4 show HRTEM images of the part as arrowed in Figure 4d; the average interplanar spacing in the quadrate frame is 0.25 nm, which is close to the lattice spacing between every (311) plane of the fcc Fe$_3$O$_4$ crystal (0.253 nm). Combined with the SAED results, it is concluded that Fe$_3$O$_4$ nanoparticles are in single-crystalline nature. The TEM image of Sample 1 obtained after the acid treatment process (see Figure 4h) indicates that they are in hollow tube-like forms, and their interior part consists of many hollow compartments separated with graphite layers, which look like bamboo too. These graphite layers are generally found in the thinner parts of whole CMTs and their hollow compartments are spaced at different separations, which is consistent with the TEM observation analyses results of the BCIOs (without utilizing the acid treatment process). Figure 4i presents a magnified TEM image of the part as arrowed in Figure 4h; the inset corresponds to the SAED pattern, in which only diffused arcs and 002 diffraction rings could be observed, which could be ascribed to the diffraction of graphite. The TEM observation results of Sample 2 indicated that the finally as-obtained product consists of Fe$_3$O$_4$ particles embedded in irregular shaped carbon capsules and form core−shell composites. A representative TEM image of Sample 2 (after acid treatment) shown in Figure 4j reveals that only irregular shaped hollow carbon capsule materials could be observed.

Discussion

When comparing our previous experimental results with the present ones, a question involuntarily emerged, that is, why the finally as-produced Fe$_3$O$_4$ encapsulated in carbon core−shell composites have quite different characteristics. It is concluded that these phenomena could be ascribed to the different structures of glycerol and ethanol to some extent. When the same volumes (18 mL) of glycerol and ethanol were used as solvents in these experiments, respectively, the former experiment could create more OH$^-$ than the latter one during the reaction process, that is to say, with gradually elevated temperature, the former experiment would produce more H$_2$O molecules from the interaction of glycerol than the latter (ethanol) at a certain temperature; however, excessive H$_2$O molecules produced in the present experiment were considered not favor for the formation of Fe$_3$O$_4$ nanowires, but agglomerated Fe$_3$O$_4$ clusters. The possible formation processes of these Fe$_3$O$_4$ encapsulated in CMTs were proposed as follows (their schematic growth models are shown in Figure 5): at first, iron nanoparticles were released by the decomposition of ferrocene, which acts as an effective and necessary dehydrogenation catalysts in these experiments. When ethanol was used as
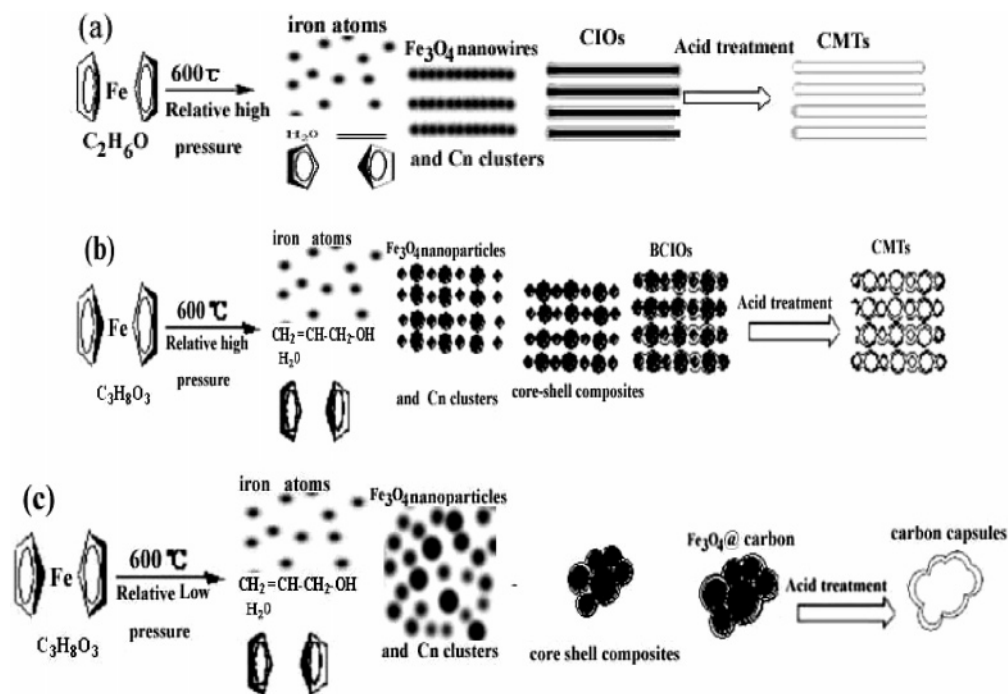
Figure 5. Schematic growth models of the as-obtained different shaped Fe_3O_4 encapsulated in carbon core−shell composites and hollow carbon materials.

solvent, the as-formed iron nanoparticles would gradually react with H_2O to form Fe_3O_4 nanoparticles and gradually develop into 1D Fe_3O_4 nanowires under relatively high reaction pressure (when the filling ratio was about 90%); finally Fe_3O_4 nanowires fully encapsulated in CMTs core−shell composites were formed with the continued deposition and diffusion of carbon atoms on their surface (as illustrated in Figure 5a). When glycerol was used as solvent, the iron nanoparticles first decomposed from ferrocene were accelerated to react with abundant H_2O molecules to form Fe_3O_4 nanoparticles in advance. These as-formed Fe_3O_4 nanoparticles and clusters (agglomerating with each other) were speedy wrapped by a small number of carbon atoms (forming a thin carbon lamella) to reduce their surface energy, and form Fe_3O_4 particles encapsulated in thin carbon capsules; these thin carbon lamella confined the continued growth of inner Fe_3O_4 nanoparticles into Fe_3O_4 nanowires, and they were self-assembled into 1D composites under the relatively high pressure (when the filling ratio was about 90%) and their interacted magnetisms. As the amount of released carbon atoms in these experiments is in excess, the continued addition (or diffusion) of carbon as atoms, chains, and rings[24] finally leads to the formation of bamboo-shaped Fe_3O_4 particles encapsulated in CMTs (see Figure 5b). And it is reasonable to consider that these core−shell composites tend to form irregular shaped Fe_3O_4 particles encapsulated in carbon capsules (see Figure 5c) when the experiment was carried out under relatively low pressure (when the filling ratio was about 30%).

Besides the reactants, it was found that the reaction pressure, temperature, and homogenization degrees of the reactants also play important roles in the final shapes of the product: First, when the experiment was carried out under relatively low pressure (when the filling ratio was about 30%), the as-obtained products were mainly composed of irregular shaped Fe_3O_4 particles embedded in carbon core−shell composites, and their typical TEM image of the corresponding product obtained after the acid treatment process is shown in Figure 4j. While 1D BCIOs composites were obtained only at relative high pressure (when the filling ratio was about 90%), therefore, it is evident

that the relatively high reaction pressure was favorable for the growth of 1D Fe_3O_4 encapsulated in carbon core−shell composites. Second, the reactants should be mixed homogeneously, otherwise, only irregular shaped carbon-related materials could be produced. Third, in this experiment, the temperature of the electronic furnace was gradually raised from room temperature to 600 °C; this point was considered favorable for the final formation of the BCIOs core−shell composite. When the initiative experimental temperature was directly set at 600 °C, we could not obtain regular shaped products.

Conclusion

In summary, one-dimensional bamboo-shaped Fe_3O_4 particles encapsulated in carbon microtubes (BCIOs) have been in situ synthesized by solvothermal pyrolysis of ferrocene and glycerol mixtures in a stainless steel autoclave, and bamboo-shaped carbon microtubes were obtained after the acid treatment process. These BCIOs have wide and periodic variable outer diameter distributions and have lengths up to tens of micrometers. The magnetic property of the BCIOs was studied and it was found that their coercivity values were in inverse ratio with the sizes of interior Fe_3O_4 particles when compared with previous reports, and their possible growth mechanism is proposed based on the experimental results. The synthetic route with ferrocene and ethanol or glycerol as reactants in a sealed autoclave has been proved to be an effective one for producing Fe_3O_4/carbon core−shell composites and it might be a preferred choice to be applied to prepare many other novel core−shell and hollow carbon related materials when ferrocene and different C−H−O systems (meaning the compounds contain alcoholic hydroxyls and alkyls) are used as reactants in a sealed autoclave.

References and Notes

(1) Pradhan, B. K.; Toba, T.; Kyotani, T.; Tomita, A. *Chem. Mater.* **1998**, *10*, 2510−2515.

Fe$_3$O$_4$ Particles in Bamboo-Shaped Carbon Microtubes

J. Phys. Chem. B, Vol. 110, No. 9, 2006 **3875**

(2) Flahaut, E.; Peigney, A.; Laurent, Ch.; Marliere, Ch.; Chastel, F.; Rousset, A. *Acta Mater.* **2000**,*48*, 3803−3812.

(3) Cornell, R. M.; Schwertmann, U. *The Iron Oxides*: *Structure*, *Properties*, *Reactions*, *Occurrence and Uses*; VCH: New York, 1996.

(4) Raj, K.; Moskowitz, B.; Casciari, R. *J. Magn. Magn. Mater.* **1995**, *149*, 174−180.

(5) Van der Zaag, P. J.; Bloemen, P. J. H.; Gaines, J. M.; Wolf, R. M.; Van der Heijden, P. A. A.; Van de Veerdonk, R. J. M.; De Jonge, W. J. M. *J. Magn. Magn. Mater.* **2000**, *211*, 301−308.

(6) Hafeli U.; et al. *Scientific and Clinical Applications of Magnetic Microspheres*; Plenum Press: New York, 1997.

(7) Bonnemain, B. *J. Drug Targeting* **1998**, *6*, 167.

(8) Jiang, L. Q.; Gao L. *Chem. Mater.* **2003**, 15, 2848−2853.

(9) Baughman, R. H.; Zakhidov, A. A.; Heer, W. A. de *Science* **2002**, *297*, 787−792.

(10) Dai, H. *Surf. Sci.* **2002**, *500*, 218−241.

(11) Saito, Y.; Yoshikawa, T. *J. Cryst. Growth* **1993**, *134*, 154−156.

(12) Saito, Y. *Carbon* **1995**, *33* (7), 979−988.

(13) Li, D. C.; Dai, L. M.; Huang, S. M.; Mau, A. W. H.; Wang, Z. L. *Chem. Phys. Lett.* **2000**, *316*, 349−355.

(14) Mariane, C. S.; Marcela, M. O.; Daniel, U.; Aldo, J. G. Z. *Chem. Phys. Lett.* **2003**, *381*, 541−548.

(15) Kovalevski, V. V.; Safronov, A. N. *Carbon* **1998**, *36* (7−8), 963−968.

(16) Lee, C. J.; Park, J. *Appl. Phys. Lett.* **2000**, *77*, 3397−3399.

(17) Murakami, H.; Hirakawa, M.; Tanaka, C.; Yamakawa, H. *Appl. Phys. Lett.* **2000**, *76* (13), 1776−1778.

(18) Ma, X.; Wang, E. G. *Appl. Phys. Lett.* **2001**, *78* (7), 978−980.

(19) Xu L. Q.; Zhang, W. Q.; Ding, Y. W.; Peng, Y. Y.; Zhang, S. Y.; Yu, W. C.; Qian, Y. T. *J. Phys. Chem. B* **2004**, *108* (30), 10859−10862.

(20) Xu L. Q.; Liu, J. W.; Du, J.; Peng, Y. Y.; Qian, Y. T. *Carbon* **2005**, *43* (7), 1563−1565.

(21) Si, S. F.; Li, C. H.; Wang, X.; Yu, D. P.; Peng, Q.; Li, Y. D. *Cryst. Growth Des.* **2005**, *5* (2), 391−393.

(22) Kodama, R. H.; Berkowitz, A. E.; McNiff, E. J.; Foner, S. *Phys. Rev. Lett.* **1996**, *77*, 394−397.

(23) Arajs, S.; Amin, N.; Anderson, E. E. *J. Appl. Phys.* **1991**, *69* (8), 5122−5123.

(24) Rao, C. N. R.; Govindaraj, A.; Sen, R.; Satishkumar, B. C. *Mater. Res. Innovations* **1998**, *2*, 128−141.